JCTC Journal of Chemical Theory and Computation

Electronic Continuum Model for Molecular Dynamics Simulations of Biological Molecules

I. V. Leontyev and A. A. Stuchebrukhov*

Department of Chemistry, University of California Davis, One Shields Avenue, Davis, California 95616

Received November 2, 2009

Abstract: Electronic polarizability is an important factor in molecular interactions. In the conventional force fields such as AMBER or CHARMM, however, there is inconsistency in how the effect of electronic dielectric screening of Coulombic interactions, inherent for the condensed phase media, is treated. Namely, the screening appears to be accounted for via effective charges only for neutral moieties, whereas the charged residues are treated as if they were in a vacuum. As a result, the electrostatic interactions between ionized groups are exaggerated in molecular simulations by a factor of about 2. The model discussed here, MDEC (Molecular Dynamics in Electronic Continuum) provides a theoretical framework for modification of the standard nonpolarizable force fields to make them consistent with the idea of uniform electronic screening of partial atomic charges. The present theory states that the charges of ionized groups and ions should be scaled, i.e., reduced by a factor of about 0.7. In several examples, including the interaction between Na^+ ions, which is of interest for ion-channel simulations, and the dynamics of an important salt bridge in cytochrome *c* oxidase, we compared the standard nonpolarizable MD simulations with MDEC simulations and demonstrated that the MDEC charge scaling procedure results in more accurate interactions. The inclusion of electronic screening for charged moieties is shown to result in significant changes in protein dynamics and can give rise to new qualitative results compared with the traditional nonpolarizable force fields simulations.

1. Introduction

At present, the majority of molecular dynamics simulations are performed by using nonpolarizable models such as AMBER,[1,2] CHARMM,[3] GROMOS,[4] and OPLS.[5] Presumably, the effects of electronic polarization and screening of electrostatic interactions are incorporated in the effective charges and other empirical parameters of the force fields; however, the extent to which this is so has never been entirely clear. [Throughout the paper the term "electronic screening" means a reduction of the electric field and electrostatic interactions due to an electronic relaxation of the environment. The origin of the effect is discussed elsewhere, e.g., in ref 6.] The importance of electronic polarizability is well recognized: for example, roughly half of the solvation free energy of ions is due to electronic polarization of the medium, and the interaction between charges is roughly half as weak, due to only electronic screening compared with that in a vacuum; therefore a significant effort is being undertaken to develop accurate fully polarizable force fields for biomolecules, see, e.g., refs 7–14.

Yet, in many cases, nonpolarizable models have been remarkably successful in modeling complex molecular systems.[15] For example, the properties of liquid water are described quite accurately without introducing electronic polarizability explicitly; likewise, the hydration free energies can be computed quite accurately using nonpolarizable simulations.[16] On the other hand, the simulation of polarization effects in low-polar solvents, e.g., ethers,[14] and especially in nonpolar solvents, e.g., alkanes,[13,17] meets serious problems. The nonpolarizable models can also significantly underestimate the magnitude of the dielectric response in a low-dielectric interior protein environment. For example, the dielectric constant of the inner part of cytochrome *c* was found to be only about 1.5,[18] which is lower than pure

* Corresponding author e-mail: stuchebr@chem.ucdavis.edu.

10.1021/ct9005807
Published on Web 04/08/2010

electronic dielectric constant $\varepsilon_{el} \cong 2.0$.[19] Many other shortcomings of nonpolarizable MD simulations have been recently discussed in the literature, see ref 20 and references therein.

The polarizable models aim at resolving the problems mentioned above. Most of such models involve various kinds of coupled polarizable sites[7–14] and the computationally expensive procedure of achieving self-consistency of polarization of such sites at each molecular dynamics time step. Although, with the Extended-Lagrangian technique,[7,11–14] the computation cost of polarizable simulations can be significantly reduced, the implementation of such models is yet to be completed; at present, even the simplest classical Drude oscillator model[11–14] is still not readily available for application to many biological systems.

As fully polarizable force fields are being developed, there is also a growing interest in improving the existing empirical nonpolarizable models to capture more accurately the effects of electronic polarization and screening in MD simulations. Given a specially designed (but empirical in nature) procedure of how the partial charges are selected,[1–3] the charges of neutral residues do reflect, at least approximately, the effects of electronic screening—in a way, how, for example, TIP3P or similar fixed-charge models of water do. One issue of concern, however, is that the electrostatic interactions of ions are described in standard nonpolarizable force fields, such as CHARMM or AMBER, by their original integer charges (e.g., $\pm$ 1, for Na^+ and Cl^-), i.e., as if these ions were in a vacuum, completely disregarding the effect of electronic dielectric ($\varepsilon = \varepsilon_{el}$) screening inherent to the condensed phase medium. The interaction of such bare charges obviously is overestimated by a factor of about 2 (the screening factor ε_{el} is about 2 for most of organic media[13]). Thus, in simulation of ion channels ions (e.g., several K^+ ions in the same channel, just a few angstroms apart) interact very strongly, and therefore their interactions are important to describe correctly (see, e.g., ref 21) or, for interaction of the ions with water molecules or other partial atomic charges of the protein, for that matter. The same is true for *charged* residues in the protein, such as Arg^+ or Glu^-, partial charges of which carry their original net values $\pm$1. The use of the bare charges in nonpolarizable simulations would be appropriate for a vacuum, but not for the condensed phase, where all charges are essentially immersed in the electronic continuum, which weakens their interactions by about a factor of 2—a typical electronic (or high-frequency) dielectric constant ε_{el} of any organic material.

Given the phenomenological nature of the force fields, one can argue that, in fact, partial charges should be considered only as formal parameters. However, they are often used, for example, in hybrid QM/MM calculations, where one needs to evaluate the electric field of the protein medium to which the QM system is exposed. The use of CHARMM or AMBER charges in such calculations has become standard and has been adopted in many studies.[22,23] Obviously, the electric potential of the charges should reflect the electronic screening of the medium.

One may also think that the atomic charges, dipoles, etc. are chosen in the force fields in such a way as to make the medium "over-polarized"[14] so that the effective nuclear relaxation/polarization alone would reflect both the effects of electronic and actual nuclear polarization. In this case, however, there is a question of relaxation time scale: on the time scale of nuclear motion, the electronic polarization and screening occurs almost instantaneously, reducing at once all electrostatic interactions by a factor of 2, whereas the effective polarization evolves on the time scale of the nuclear motions.

The question arises then as to whether it is possible to introduce an appropriate scaling of bare charges of ionized groups and ions to correctly reflect the electronic screening? Here, we argue that the bare charges of the ionic groups can and should be scaled, in particular when the electrostatic potentials of such groups are considered.

More generally, we discuss a principle of uniform charge-scaling based on which one could systematically build a nonpolarizable force field for simulations of condensed media. The principle is based on a simple idea of a uniform electronic continuum, with an effective dielectric constant $\varepsilon \sim 2$, and point charges moving in it. The resulting model, which combines a nonpolarizable (fixed-charge) force field for nuclear dynamics (MD) with a phenomenological electronic continuum (EC) is referred to as MDEC (Molecular Dynamics in Electronic Continuum). In this model, the effects of electronic screening are reduced to simple scaling of the partial charges. The model is similar but not equivalent to standard nonpolarizable force fields used in most MD simulations; we propose a simple scaling procedure that makes nonpolarizable force fields such as AMBER and CHARMM uniformly consistent with the idea of electronic screening, which naturally improves the quality of these force fields.

Several examples of MDEC calculations and the effects of electronic polarization will be discussed, including the interaction between Na^+ ions, which is of interest for ion-channel simulations, and the dynamics of an important salt bridge in cytochrome *c* oxidase.

2. MDEC Model

A detailed discussion of the MDEC model is given in previous publications.[24,25] Here, we restate main features of the model essential for subsequent calculations.

2.1. Screening Effect and Effective Charges. As frequently stated in the literature,[26] the partial atomic charges of nonpolarizable models, e.g., TIP3P[27] or SPC/E,[28] empirically incorporate the effect of electronic polarization in molecular interactions. There are different aspects of electronic polarization, however, that differently affect electrostatic interactions between individual molecules. Thus, the molecular dipole moment enhancement, usually considered[1–3,26] in the context of the electronic polarization, increases a strength of electrostatic interactions. On the other hand, the effect of electronic dielectric screening results in the reduction of the electrostatic interactions. Both factors are important for interaction of noncharged molecules; however, for interactions of ions, or ionized groups, where the direct Coulomb interaction dominates, the screening of

the Coulomb interaction is of prime importance. Here, the screening effect will be described in terms of charge scaling.

Consider two ions, Q_1 and Q_2, in a solvent modeled by the dielectric of ε; the charges are located at the center of spheres with corresponding ionic radii, R_1 and R_2 (no dielectric inside the spheres), and separated by the distance r. An effective interaction between these ions is given by the potential of mean force (PMF):

$$\mathrm{PMF} \equiv U^{\mathrm{eff}}(r) = \Delta G(r) - \Delta G(\infty) \tag{2.1}$$

where $\Delta G = \Delta G_{\mathrm{vac}} + \Delta G_{\mathrm{solv}}$ is the total free energy of the system (ion pair + solvent) composed of its vacuum (no solvent, ΔG_{vac}) and solvation (ΔG_{solv}) components; $\Delta G(\infty)$ is the sum of free energies of individual ions. The gradient of PMF $U^{\mathrm{eff}}(r)$ over r gives the effective force acting between ions Q_1 and Q_2 in the medium. Since we are interested in only electrostatic interactions, nonelectrostatic components of the free energies will be neglected. In the case when $r > R_1 + R_2$, the solvation free energy of the ion pair in the dielectric is accurately approximated by the well-known relation (15) from ref 29 and PMF is obtained as[29]

$$U^{\mathrm{eff}}(r) = \frac{Q_1 Q_2}{\varepsilon r} \tag{2.2}$$

which shows that Coulomb interactions are reduced (screened) by a factor $1/\varepsilon$ due to relaxation of the polarizable environment. A more detailed treatment of the origin of the screening effect is given, e.g., in ref 6 and also in ref 25.

The magnitude of the screening factor ε depends on which part of the medium relaxation is considered explicitly (as moving charges q_i) and which part is described phenomenologically as a polarizable dielectric.[30] Since in nonpolarizable microscopic models the atomic motions are described explicitly, the screening factor should include only the electronic component of the medium polarization, $\varepsilon = \varepsilon_{\mathrm{el}}$. The static (i.e., time-independent) dielectric approximation in this case is quite accurate, because on the time scale of nuclear motion the electronic polarization occurs almost instantaneously, reducing at once all interatomic electrostatic interactions by a factor of $\varepsilon_{\mathrm{el}}$. The phenomenological parameter $\varepsilon_{\mathrm{el}}$ is known from the experiment as a high-frequency dielectric permittivity ($\varepsilon_{\mathrm{el}} = n^2$, where n is a refraction index of the medium) and typically is about 2. The resulting model, which combines a nonpolarizable (fixed-charge) force field for nuclear dynamics (MD) and a phenomenological electronic continuum (EC) for the electronic polarization is referred to as MDEC.[25]

The MDEC model[25] considers charges q_i moving in an electronic polarizable continuum of known dielectric constant $\varepsilon_{\mathrm{el}}$. In the uniform dielectric, all electrostatic interactions are scaled by a factor $1/\varepsilon_{\mathrm{el}}$. Since interactions are quadratic in charges, the effect of electronic dielectric screening can be taken into account implicitly by using scaled partial charges, $q_i^{\mathrm{eff}} = q_i/\sqrt{\varepsilon_{\mathrm{el}}}$; in this case, the Coulomb interaction between sites i and j automatically has the correct form $q_i^{\mathrm{eff}} q_j^{\mathrm{eff}}/r_{ij} = q_i q_j/\varepsilon_{\mathrm{el}} r_{ij}$ without explicitly introducing factor $1/\varepsilon_{\mathrm{el}}$. The unscaled original charges q_i are difficult to specify a priori in general (they are not the same as partial charges of a condensed medium molecule in a vacuum, see ref 25), unless one deals with ions or ionized groups in a protein, whose unscaled net charges are known. But charges q_i^{eff} can be found empirically by fitting experimental data[27,28] or scaled ab initio interaction energies.[3]

2.2. Solvation Free Energy. In the MDEC model, when the solvation free energy of a group is considered, the electronic polarization free energy is treated explicitly. The free energy consists of the nuclear part ΔG_{nuc} evaluated by MD and the pure electronic polarization energy part ΔG_{el} evaluated by using the polarizable continuum model[31] (i.e., by solving the Poisson equation with corresponding boundary conditions, with dielectric constant $\varepsilon = 1$ inside the solute region and $\varepsilon = \varepsilon_{\mathrm{el}}$ outside):

$$\Delta G = \Delta G_{\mathrm{nuc}} + \Delta G_{\mathrm{el}} \tag{2.3}$$

Such an approach to electrostatic solvation free energy calculations, eq 2.3, was shown to work well both in high- and low-dielectric media[24,32] and will be further elaborated in this paper.

When the interaction of a solute with solvent molecules is considered in an MDEC simulation (in evaluating the ΔG_{nuc} part), the solute partial charges (found in an appropriate quantum-mechanical calculation, in a vacuum, or in a dielectric environment) should be scaled by $1/\sqrt{\varepsilon_{\mathrm{el}}}$, like all other charges when the forces between atoms are considered. If no scaling of solute charges was employed in the MD simulation, which is typical for standard MD simulations, see e.g. refs 16 and 33, the free energies obtained from MD, ΔG_{MD}, should be corrected directly afterward. Since in the linear response approximation the solvation free energy is quadratic in charges of the solute, ΔG_{MD} should be corrected by a factor $1/\varepsilon_{\mathrm{el}}$, giving $\Delta G_{\mathrm{nuc}} = \Delta G_{\mathrm{MD}}/\varepsilon_{\mathrm{el}}$. The total MDEC polarization free energy of the medium then is

$$\Delta G = \frac{1}{\varepsilon_{el}} \Delta G_{\mathrm{MD}} + \Delta G_{\mathrm{el}} \tag{2.4}$$

where ΔG_{MD} as stated above is the electrostatic solvation free energy obtained in nonpolarizable MD using unscaled solute charges (standard approach) and ΔG_{el} is the pure electronic part of the free energy. A more detailed description of the free energy simulation technique accounting for the electronic polarization can be found in refs 24 and 25.

2.3. Dielectric Constant of the Medium. The dielectric constant of the medium is often employed in the continuum electrostatic calculations, e.g., for solvation free energy evaluation. In microscopic calculations, on the other hand, the solvation free energy is obtained directly from MD simulations. The question arises often as to what is the effective dielectric constant of the medium, $\varepsilon_{\mathrm{MD}}$, that corresponds to a specific microscopic model of the system. The free energy relationships discussed in the previous section allow one to make a connection between the total (static) dielectric constant, ε_0, which includes both nuclear and electronic polarization effects, and the dielectric constant of nonpolarizable MD simulations, $\varepsilon_{\mathrm{MD}}$, which does not explicitly describe pure electronic polarization of the medium.

Suppose we consider a spherical ion or a pair of spherical ions; in this case, according to ref 29, the solvation energies

will be proportional to their corresponding Born factors: $\Delta G \sim (1 - 1/\varepsilon_0)$, $\Delta G_{el} \sim (1 - 1/\varepsilon_{el})$ and $\Delta G_{MD} \sim (1 - 1/\varepsilon_{MD})$. Using eq 2.4 for the relationship between these free energies, we find

$$\varepsilon_0 = \varepsilon_{MD} \cdot \varepsilon_{el} \tag{2.5}$$

That is, the total dielectric constant of the medium ε_0 is not equivalent to that reproduced by the (nonpolarizable) MD simulation, ε_{MD}; instead, the relationship between the two is given by the above formula. This indeed has been directly demonstrated[25] for several systems.

The above relation can be also obtained using a well-known expression[34] for the static dielectric constant:

$$\varepsilon_0 = \varepsilon_{el} + \frac{4\pi}{3Vk_BT}\langle M^2\rangle \tag{2.6}$$

Here, $\langle M^2\rangle$ is the mean square fluctuation of the total dipole of the dielectric sample V; k_B and T are the Boltzmann constant and temperature, respectively. According to the MDEC scaling procedure, the actual dipole moment μ of particles in the bulk is related to the effective moment μ^{eff} of these particles in the nonpolarizable model as $\mu = \sqrt{\varepsilon_{el}}\mu^{eff}$; therefore, $\langle M^2\rangle = \varepsilon_{el}\langle M_{MD}^2\rangle$, where $\langle M_{MD}^2\rangle$ is the mean square fluctuation of the dipole moment observed in a nonpolarizable MD. Thus, eq 2.5 is obtained from eq 2.6 by noticing that ε_{MD} is defined via fluctuation $\langle M_{MD}^2\rangle$ with $\varepsilon_{el} = 1$ in eq 2.6.

Although the simple relation between dielectric constants eq 2.5 was derived using arguments strictly valid only for spherical ions, and for the bulk solvent modeled with periodic boundary conditions,[34] eq 2.5 is in fact more general and provides a good estimate of the static dielectric constant ε_0 in a wide range of different solutes.[18,35]

3. Applications of MDEC Model

3.1. Water Models. Many nonpolarizable force fields are essentially MDEC models. For example, TIP3P[27] or SPC/E[28] and similar models of water involve empirical charges that can be considered as scaled charges. TIP3P is particularly interesting in this regard as it is often used in biological simulations, and it serves as a reference for phenomenological parameter assignments of CHARMM.[3]

It is known that the dipole moment of a water molecule in a vacuum is 1.85D; in the liquid state, however, the four hydrogen bonds to which each water molecule is exposed on average strongly polarize the molecule, and its dipole moment falls somewhere in the range of 2.9D to 3.2D.[36–38] [It is recognized that in ab initio simulations of bulk water the water dipole cannot be defined unambiguously and depends on the partitioning scheme used;[39] as such, its actual value remains a matter of debate. Here, we rely upon calculations and the partitioning scheme of refs 37 and 38.] The significant increase of the dipole from $\mu_0 = 1.85$D to a value $\mu \approx 3$D, or even larger, is also supported by the Kirkwood−Onsager model,[40] see the Appendix, which estimates the enhanced polarization of a molecule due to the reaction field of the polarized environment. Yet, the dipole moment of the TIP3P water model is only 2.35D. The specific value of the TIP3P dipole moment can be understood as a scaled dipole, so that the dipole−dipole interactions are screened by the electronic continuum by a factor $1/\varepsilon_{el}$. Indeed, if each dipole (or all partial charges) is scaled by a factor $1/\sqrt{\varepsilon_{el}}$, one could consider interaction of the effective dipoles, $\mu^{eff} = \mu/\sqrt{\varepsilon_{el}} \simeq 2.35$D (for water $\varepsilon_{el} = 1.78$), as if they were in a vacuum. This appears to be exactly what the fixed-charge water models do. Thus, charges of the TIP3P water model should be understood as scaled charges that reflect the effect of electronic screening.

The scaled nature of charges of the TIP3P water model is important to bear in mind when the interaction of such water models with a solute is considered. For example, if the charge of say a Na^+ ion is assigned to be +1 in a simulation, then it is obviously inconsistent with the charges of the water model, as the latter are scaled by a factor of $1/\sqrt{\varepsilon_{el}}$, while the charge of the ion is not. Clearly the strength of the interaction is overestimated in this case by a missing factor of $1/\sqrt{\varepsilon_{el}}$, i.e., about 0.7 (for proteins $\varepsilon_{el} \sim 2$). The problem would not arise if the charge of the ion were appropriately scaled. (The reason why a seemingly incorrect charge gives reasonable aqueous solvation free energy is explained next.)

3.2. Conventional Force Fields. The conventional nonpolarizable force fields of AMBER,[1,2] CHARMM,[3] GROMOS,[4] or OPLS[5] are built on different principles than those discussed in this paper; yet the atomic partial charges of noncharged groups can be understood approximately as "scaled MDEC charges", because these empirical parameters were chosen in such a way as to reflect the condensed matter nature of the interaction. For example, in CHARMM, TIP3P water (an effective MDEC model) was used as a reference in the empirical procedure[3] of setting partial charges. In contrast, the charges of ionized groups *do not* reflect the effects of electronic screening.

In free energy simulations with nonpolarizable force fields (and unscaled charges), the pure electronic contribution to the electrostatic free energy is often completely ignored, as e.g. in refs 16 and 33. Yet, in many cases, such simulations pretty accurately reproduce experimental solvation energies; this may appear surprising, given the fact that about half of the total solvation free energy (for charged solutes typically 25−50 kcal/mol) comes from electronic polarization of the medium. In fact, the neglect of large electronic polarization free energy is almost completely compensated by the use of "incorrect" bare solute charges in such simulations. This fortuitous compensation of errors, however, occurs only in the high-dielectric media, as can be seen from the following argument.

Consider for example the Born solvation energy of Na^+ ion, $Q = +1$, in water; in simulations, one would have approximately

$$\Delta G = \frac{Q^2}{2R}\left(1 - \frac{1}{\varepsilon_{MD}}\right) \tag{3.1}$$

where ε_{MD} is the dielectric constant of water that corresponds to a specific MD model employed in the calculation. No matter which model of water is used, ε_{MD} is much larger than unity; hence, the overall estimate of the solvation free

energy is $Q^2/2R$, which is independent of properties of the solvent and can match pretty well the experimental value, provided the ionic radius R is chosen correctly. The interaction between two charges is taken to be then Q^2/r, completely disregarding the electronic screening of the interaction.

The MDEC model suggests instead that in MD simulations the charge Q should be scaled, *and* the electronic solvation free energy $\Delta G_{el} = Q^2/2R(1 - 1/\varepsilon_{el})$ is added explicitly. In this case, the nuclear part of the free energy calculated in MD will be $[(Q/\sqrt{\varepsilon_{el}})^2/2R](1 - 1/\varepsilon_{MD})$ and the total free energy, eq 2.3, is given by

$$\Delta G = \frac{(Q/\sqrt{\varepsilon_{el}})^2}{2R}\left(1 - \frac{1}{\varepsilon_{MD}}\right) + \frac{Q^2}{2R}\left(1 - \frac{1}{\varepsilon_{el}}\right) \quad (3.2)$$

Since $\varepsilon_{MD} = \varepsilon_0/\varepsilon_{el}$, the above expression correctly reproduces the expected result $Q^2/2R(1 - 1/\varepsilon_0)$. Notice that the charge is not scaled when the solvation is calculated in an electronic continuum. Notice also that it is only when $\varepsilon_{MD} \gg 1$ that the two expressions 3.1 and 3.2 approximately give the same result. Yet, for the interaction energy of two charges, the MDEC gives the correct expression $Q^2/r\varepsilon_{el}$, while the standard approach gives Q^2/r.

Given that the unscaled relation (eq 3.1) is only formally correct when $\varepsilon_{MD} = \varepsilon_0/\varepsilon_{el} \gg 1$, it is not surprising that the pure nonpolarizable approach works well in aqueous solutions ($\varepsilon_0/\varepsilon_{el} \sim 40$), as e.g. in refs 16 and 24; however, the approach fails (i.e., significantly underestimates the polarization effects) in low dielectric media ($\varepsilon_0/\varepsilon_{el} \sim 1$) as in refs 13, 14, and 41–43.

In contrast, an MDEC simulation of polarization effects is correct for both high- and low-dielectric media, as shown in the modeling of hydration free energies of ions,[24] dielectric constants of neat alcohols, alkanes,[25] and protein interiors of cytochrome *c* and cytochrome *c* oxidase[44] as well as nonequilibrium reorganization energies in water, dichloroethane, tetrahydrofuran, and supercritical carbon dioxide solvents.[32]

We next show that despite a complex nature of electronic polarization in a real system, the effect in practice can be described reasonably well by a simple charge scaling procedure; this opens a way to modify the standard force fields so as to improve the description of their charged groups by effectively incorporating the electronic screening of charges.

3.3. Ab Initio Interactions Modeled by Charge Scaling. Here, we consider the interaction of several charged species in ab initio calculations. The ab initio treatment captures the effects of electronic polarization of charged species themselves, while the effects of the polarization of the environment, and corresponding screening, are described here phenomenologically, by a continuum with dielectric $\varepsilon_{el} = 2.0$.

The interaction energies were calculated using a quantum-mechanical procedure identical to that of the CHARMM parametrization protocol,[3] with amino acids substituted by their corresponding model compounds (glutamate by propionate and arginine by *n*-propyl guanidinium). The isolated model compounds were optimized at the HF/6-31G(d) level.

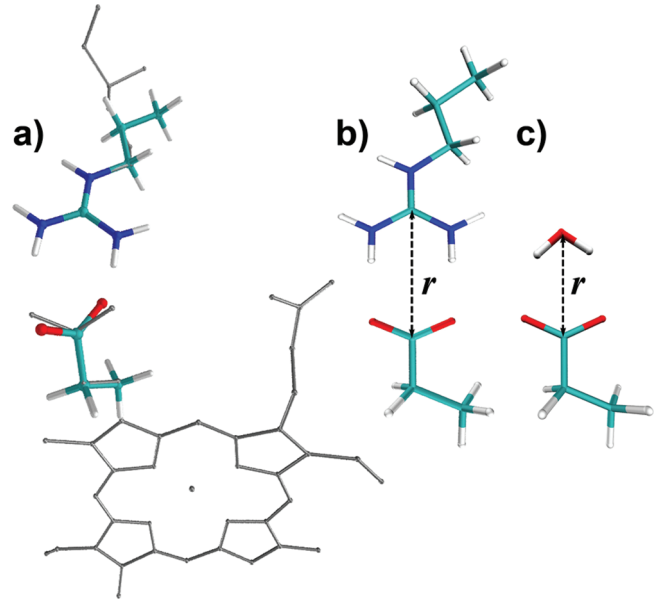

Figure 1. Mutual orientation of model compounds. (a) The initial configuration of the Glu^- and Arg^+ model compounds corresponds to the position of the salt bridge Arg438A−PropD of heme a_3 in cytochrome *c* oxidase (see section 3.5). (b) The optimized configuration of Glu^- and Arg^+ model compounds. (c) The optimized configuration of the Glu^- model compound and a water molecule. The interaction distance *r* is shown for optimized structures.

The optimized structures were then used to construct compound "supermolecules" consisting of a model compound and a single water molecule (or another compound). The supermolecule structures were optimized at the HF/6-31G(d) level by varying the interaction distance *r* and mutual angles, to find the optimum position with fixed monomer geometries. The mutual orientations of the model compounds in the supermolecules are shown for the interacting pairs Arg^+-Glu^- and $Glu^-{-}H_2O$ in Figure 1. The mutual angles were then fixed while the interaction distance *r* was varied. For each structure with a given *r*, the interaction energy was calculated as the difference between the total supermolecule energy and the sum of the individual monomer energies. The gas-phase interaction energies were calculated with model compounds in a vacuum, while the bulk-phase interactions were obtained with the model compounds immersed in the dielectric of $\varepsilon = 2$. The quantum-mechanical calculation in the dielectric utilized the PCM[31] technique and self-consistent reaction-field procedure implemented in Gaussian 03.[45] The PCM cavities were built using the Gaussian 03 default setup[45] for atomic radii without the generation of smoothing spheres (keyword NOADDSPH). In this united atom model, the radii of CH3, CH2, C, NH, NH2, OH2 and O are taken as 2.525 Å, 2.325 Å, 1.925 Å, 1.93 Å, 2.03 Å, 1.95 Å, and 1.75 Å, respectively. The calculations were performed with a surface grid element of 0.1 Å^2 average size.

In Figure 2a−c, the ab initio interactions between ions Na^+-Na^+ and Arg^+-Glu^- and between the Glu^- ion and water are compared with those modeled by the original and scaled CHARMM[3] force fields. (For amino acids, their corresponding model compounds are used.) In all cases, as expected, there is a significant screening effect of the

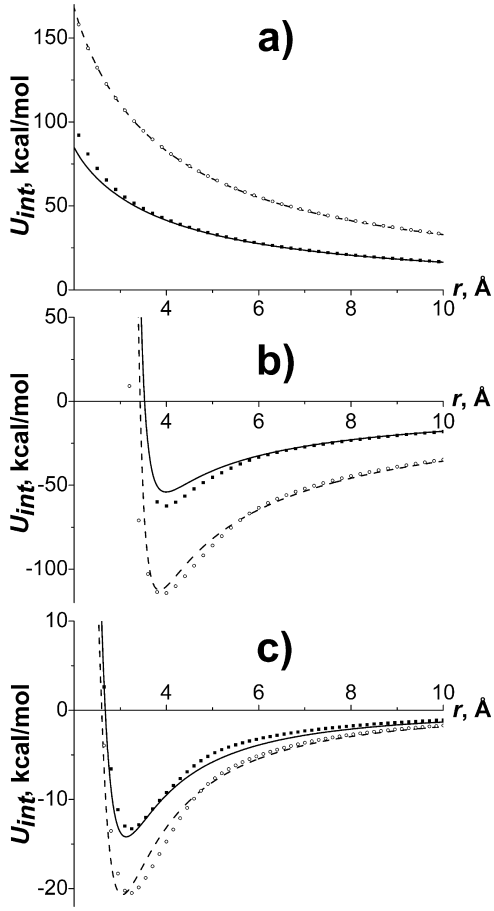

Figure 2. Interaction energies between (a) Na^+-Na^+ ions, (b) Arg^+ and Glu^- amino acids, and (c) Glu^- amino acid and water. Open circles stand for the energies obtained in the gas-phase HF/6-31G(d) calculation; filled squares are for the same interactions but calculated in the dielectric of $\varepsilon = 2.0$. The dashed lines represent interaction energies obtained by the standard CHARMM force field and using the TIP3P water model in (c). The solid lines represent the interaction energies obtained by the CHARMM force field with scaled charges ($\varepsilon_{el} = 2.0$) and the TIP3P water model in (c).

dielectric environment on the interaction energy; the effect as seen, however, can be pretty accurately reproduced by a simple scaling of charges. Notice that the charges are scaled by a factor $1/\sqrt{\varepsilon_{el}}$; in correspondence with what has been said about the TIP3P water model (section 3.1), in the example of the $Glu^-{-}H_2O$ pair, only charges of Glu^- were scaled. Notice how accurately the scaled CHARMM force field reproduces the results of ab initio calculations. Similar results are expected for other standard force fields (such as AMBER,[1,2] GROMOS,[4] etc.) where charged groups are also treated as having their original vacuum net charges.

Thus, the simple charge scaling procedure in standard nonpolarizable force fields can account for the effects of electronic screening not only in the interactions between ions but also between ions and water. Although, as seen in Figure 2a, some additional adjustments of the nonelectrostatic parameters might be useful to improve the interactions at shorter distances.

3.4. Forces between Ions in a Polarizable Environment. To test how well the phenomenological electronic continuum of the MDEC model describes a molecular

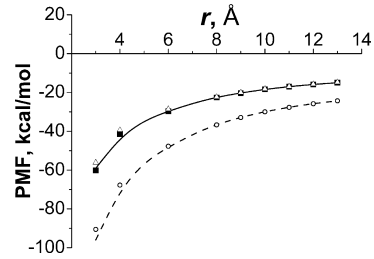

Figure 3. PMF for an ion pair A^+ and A^- in benzene. The squares, circles, and triangles stand for the MD results obtained with polarizable MD, nonpolarizable CHARMM, and CHARMM with scaled charges of the ions, respectively. Continuous curves are the least-squares fitting of the simulation points by the Coulomb function $-1/\varepsilon r$ (with the Ewald correction, see the Appendix). For polarizable simulations (solid line), the effective dielectric constant $\varepsilon = 1.88(\varepsilon_0)$ for nonpolarizable simulations (dashed line), $\varepsilon = 1.16(\varepsilon_{MD})$. The triangles correspond to *nonpolarizable* CHARMM simulations with *scaled* charges by a factor $1/\sqrt{(\varepsilon_0/\varepsilon_{MD})}$ according to the MDEC model, eq 2.3.

solvent, with its structure and corresponding inhomogeneity of electronic polarization, here we examine a model of two ions A^- and A^+ dissolved in benzene; the low-dielectric environment is chosen to model the interior of a protein, or a lipid membrane. The solvent now is described by the polarizable Drude oscillator model,[11] whereas ions are treated by a standard nonpolarizable force field (Coulomb and Lennard-Jones interactions; the LJ parameters for ions correspond to those of Cl^- ion.) For such a system, we calculate the electrostatic part of the potential of mean force as defined by eq 2.1 and compare the results with those of scaled and unscaled CHARMM calculation, using the concepts of MDEC theory, see Figure 3. The PMF gradient over r gives the average electrostatic force acting between charged particles A^- and A^+ in the bulk. The solvation free energy $\Delta G(r)$ of ions was evaluated by three alternative techniques: by polarizable MD, by the standard MD technique using a nonpolarizable CHARMM force field, and by MD using eq 2.3 and the CHARMM force field with scaled ion charges, according to the MDEC model. Further details of the simulations are given in the Appendix.

As seen in Figure 3, when the space between ionic spheres is larger than a size of solvent molecules, the effects of the solvent microscopic structure become unimportant, and the average interaction, both in polarizable and nonpolarizable models of benzene, can be approximated by a simple Coulomb law with an effective dielectric constant (obviously the LJ interactions are not important in this region). In the case of a polarizable Drude oscillator model for solvent benzene, the average interaction between ions is reproduced with an effective dielectric constant $\varepsilon_0 = 1.88$. [We notice that the experimental value of ε_0 for benzene is actually 2.3;[46] the underestimated MD value of ε_0 is a consequence of the reduced polarizability parameter employed in the benzene model,[11] which is ~20% lower than experimental benzene polarizability.]

According to MDEC theory, eq 2.5, the total dielectric constant of the medium ε_0 is a product of the electronic dielectric ε_{el} (due to Drude polarization of benzene mol-

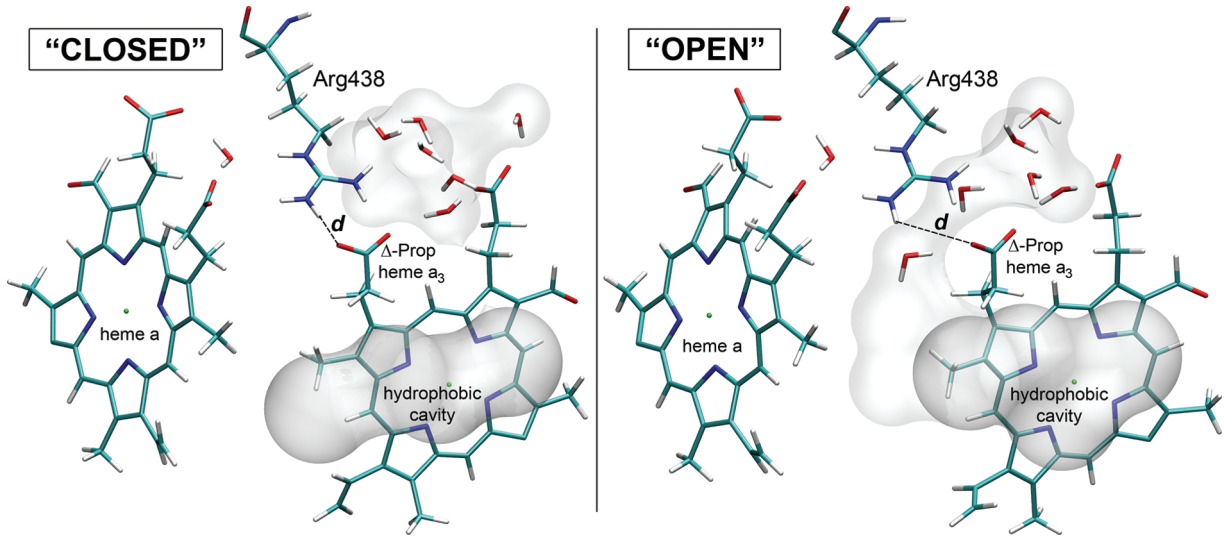

Figure 4. Salt bridge between Δ-propionate of heme a_3 and Arg438A in bovine cytochrome *c* oxidase. Configurations, when the gate is "OPEN" and "CLOSED", are shown.

ecules) and that of nuclei, ε_{MD}. The latter was obtained in a separate simulation using the nonpolarizable CHARMM model of benzene, see Figure 3 (dashed line); the corresponding value is $\varepsilon_{MD} = 1.16$. According to eq 2.5 then, the corresponding electronic dielectric constant of the polarizable model of benzene is $\varepsilon_{el} = \varepsilon_0/\varepsilon_{MD} = 1.62$. As seen in Figure 3 (solid line), in perfect agreement with MDEC theory, the results of *polarizable* benzene simulations are reproduced by scaling charges of ions (by a factor $1/\sqrt{1.62}$) and running *nonpolarizable* CHARMM simulations. Again, we see that all effects of electronic polarization can be incorporated by scaling charges of ions with a factor $1/\sqrt{\varepsilon_{el}}$.

The significant deviation of the results of standard nonpolarizable MD from those of polarizable and MDEC techniques shown in Figure 3, in fact, can be rationalized without the PMF simulations. Since the scaling of Coulomb interactions for each microscopic model is given by the corresponding dielectric constant (as defined in section 2.3), the PMF profiles are approximated by the corresponding Coulomb functions $-1/\varepsilon_0 r$, $-1/\varepsilon_{MD} r$ and $-1/((\varepsilon_{el}\varepsilon_{MD})r)$ for the polarizable, nonpolarizable CHARMM, and MDEC techniques, respectively. Due to the relation (eq 2.5), PMF functions for polarizable MD and MDEC should be the same, while deviation from the CHARMM technique is estimated as $(1 - 1/\varepsilon_{el})(1/\varepsilon_{MD} r)$. Thus, for the low-dielectric media where $\varepsilon_{el} = 2$ and $\varepsilon_{MD} \sim 1$, the deviation is $\sim 1/2r$, which is significant even for larger separation distances (~16 kcal/mol for $r = 10$ Å). In the high-dielectric media ($\varepsilon_{MD} \gg 1$), however, the difference will be much smaller. For instance, in water ($\varepsilon_{el} = 1.8$, $\varepsilon_{MD} \sim 100$ for the TIP3P model[47]), the deviation will be just $\sim 1/225r$, which is ~0.5 kcal/mol even for the shortest separation $r \leq 4$ Å (contact ion pair: $r \leq 2R_{vdW}$). Since the difference 0.5 kcal/mol is on the order of statistical uncertainty of MD, the missing electronic screening effect is not noticeable in the standard nonpolarizable simulations of water solutions.

3.5. Dynamics of Salt Bridges in Proteins. To demonstrate the significance of accounting for the electronic polarization in protein dynamics simulations, we modeled fluctuations of an important salt bridge (Arg438A−PropD of heme a_3) in cytochrome *c* oxidase (C*c*O), see Figure 4. This salt bridge (SB) controls water penetration to the hydrophobic cavity in the catalytic center of C*c*O.[48,49] The strength of the electrostatic interaction of the salt bridge determines the rate of its opening/closing and, as a result, the probability of water transfer to/from the catalytic cavity.

The distance *d* between O2D of Δ-propionate and 2HH2 of Arg438 (as shown in Figure 4) has been chosen to characterize the fluctuations of the salt bridge gate during an MD run. The AMBER[1,2] force field was used. The simulation setup is similar to that of ref 44. Details of the MD simulations are given in the Appendix. The distribution functions for distance *d* obtained with scaled and original unscaled charges are shown in Figure 5a. Here, no water in the cavity was included in the simulation.

It is seen that the SB dynamics become qualitatively different once electrostatic interactions between the charged $Arg438^+$ and the COO^- group of Δ-propionate are reduced by a factor of $1/\varepsilon_{el}$ (in the simulations, $\varepsilon_{el} = 2.0$). In contrast to the standard MD simulations,[49] the fluctuations observed in the scaled model are significantly larger, so that the internal water can now easily pass through the opened SB gate and enter the catalytic cavity. In fact, during a 5 ns MD run with scaled charges, several such water transitions were observed.

In Figure 5b, the distribution functions of *d* are shown from simulations that included water in (and around) the catalytic cavity of the enzyme. As we already pointed out, the electronic screening affects not only charge−charge interactions but interaction with water as well. Here, the TIP3P model is taken without modification; the charge scaling affects only the salt bridge groups. As seen in Figure 5b when the effects of electronic screening are included, even more dramatic changes are observed.

Thus, standard (unscaled charges) MD simulations with and without water in the cavity lead to the conclusion that the salt bridge is formed 100% of the time; here stability of the salt bridge is quantified by the criterion $d < 3$ Å, while the bridge is observed only 98% or even 63% of the time in

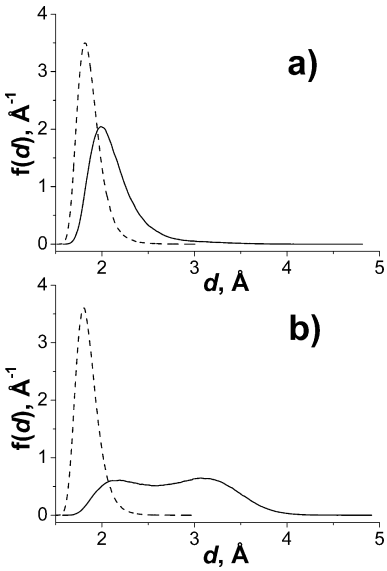

Figure 5. Distribution functions of the distance *d* between O2D (Δ-propionate of heme a_3) and 2HH2 (Arg438A) of C*c*O salt bridge: (a) no water in the catalytic cavity; (b) 4 water molecules added to the cavity. Dashed lines represent distributions obtained in the standard MD, while solid lines stand for the distributions obtained in the MD with scaled charges of the ionized groups.

simulations with scaled charges without (see Figure 5a) and with water (see Figure 5b), respectively.

It is clear that the account for electronic screening of charged groups can give rise to *qualitatively different* results in simulations of proteins. As we have shown, this can be achieved in a computationally effective way by simple charge scaling of ionized groups in the protein.

Unfortunately, there are no direct experimental data on the dynamics of the salt bridge discussed here to verify our proposal of electronic screening. However, as we argued in this paper, such a scaling is obvious from a theoretical point of view. An indirect comparison with an experiment, and support of charge scaling, is provided by some other computational studies, such as Zhu et al.,[50] where a heuristic approximation for the charge scaling of ionized side chains (variable dielectric constant ≥ 2) somewhat similar to ours was employed, which resulted in significant improvement in both side chain and loop prediction for protein conformations.

4. Conclusions

There is inconsistency in how the effect of electronic screening of Coulombic interactions, inherent for the condensed phase media, is treated in the conventional force fields such as AMBER[1,2] or CHARMM.[3] Namely, the screening appears to be accounted for via effective charges only for neutral moieties, whereas the charged residues are treated as if they were in a vacuum. As a result, the electrostatic interactions between ionized groups are exaggerated in molecular simulations by a factor of about 2.

The discussed MDEC (Molecular Dynamics in Electronic Continuum) model provides a theoretical framework within which the charge screening of both ionized and neutral residues can be achieved on the same footing. In a few examples, we compared the standard nonpolarizable MD simulations with MDEC simulations and demonstrated how the charges of ionized groups can be rescaled to correspond to the MDEC model. The present theory states that the charges of ionized groups of the protein, as well as charges of ions, in simulations with conventional nonpolarizable force fields such as CHARMM, AMBER, etc. should be scaled, i.e., reduced by a factor of about 0.7, to reflect the electronic screening of the condensed medium appropriate for biological dynamics simulations. If the charge-scaling procedure is employed, in the solvation free energy calculations, the electronic polarization energy should be treated explicitly, i.e., explicitly added to the nuclear part of the free energy, eq 2.3. *Ab initio* calculations of interaction energies (section 3.3) and MD simulations of the potential of mean force (section 3.4) indicate that the MDEC charge scaling procedure results in more accurate interactions not only between ions but also between ions and nonpolarizable water models, such as TIP3P, often used in biological simulations. Given the above examples and earlier reports,[24,25,32] we conclude that the MDEC model provides a way to more accurate modeling of condensed-phase molecular systems.

The ignored electronic screening between ions in standard MD simulations may be unnoticeable in molecular simulations of high-dielectric media such as water solutions; however, it has a dramatic effect (section 3.5) in the dynamics of charged systems such as salt bridges in a low-dielectric protein interior.

Acknowledgment. We would like to acknowledge many stimulating discussions of the subject of the paper with Professor Toby Allen of UC Davis and Dr. Igor Vorobyov. This work has been supported in part by the NSF grant PHY 0646273 and NIH GM054052.

Appendix

Kirkwood−Onsager Model of Water in the Bulk. Consider a polarizable point dipole in the middle of a sphere cut in the medium of dielectric constant ε_0; the radius of the sphere is a, the permanent dipole value (dipole of water in vacuum) is μ_0, and the dipole polarizability (i.e., electronic polarizability of water) is α. The increase of the dipole due to the reaction field of the polarized medium is[40]

$$\mu = \frac{\mu_0}{1 - \frac{\alpha}{a^3}\frac{2(\varepsilon_0 - 1)}{2\varepsilon_0 + 1}} \qquad \text{(A1)}$$

Taking $\varepsilon_0 = 78$ for the dielectric constants of water, $\mu_0 =$ 1.85D for a water dipole in a vacuum and $\alpha = 1.47$ Å^3 for the polarizability of water, for reasonable values of radius a in the range of 1.4−1.6 Å, one obtains a range of possible values of μ: 2.9−3.9D [Here the radius 1.4 Å corresponds to one-half of the most probable OO distance in the radial distribution function of bulk water, whereas 1.6 Å corresponds to one-half of the average intermolecular distance in the bulk]. Although this is a crude model, it nevertheless strongly indicates that the actual dipole of water in the bulk is much larger than the empirical value of 2.35D of the TIP3P model.

Potential of Mean Force Calculations. Consider two generic ions, A^- and A^+, with ionic radii, R^- and R^+, separated by a distance r, dissolved in polarizable benzene. In the continuum solvent approximation (in the dielectric region $r > R^- + R^+ + 2R_{solvent}$), the estimate for PMF $U^{eff}(r)$ of the ions is given by eq 2.2. If the finite system is simulated with periodic boundary conditions, then the expression (eq 2.2) should be corrected by the Ewald term:

$$U^{eff}(r) = -\frac{1}{\varepsilon r} + \frac{1}{\varepsilon}\text{Ewald}(r) \qquad \text{(A2)}$$

where Ewald(r) is the interaction of A^- and A^+ ions with all periodic images (excluding the solvent). The effective value of ε is determined by fitting the continuous expression A2 to the MD simulated PMF data.

PMF was simulated employing eq 2.1 and different microscopic models of the benzene solvent: the polarizable Drude oscillator model[11] and the nonpolarizable CHARMM[3] and MDEC models. The ions were treated by a standard nonpolarizable force field (Coulomb and Lennard-Jones interactions; the LJ parameters for ions correspond to those of the Cl^- ion[3]). The solvation free energies of the ionic pair were evaluated by the standard technique of thermodynamic integration within the linear response approximation. The MDEC free energies were calculated employing eq 2.3 and the CHARMM force field (with scaled charges of ions) for MD simulation of the nuclear part of the free energy ΔG_{nuc}. The electronic part of the free energy ΔG_{el} was estimated by solving the continuum electrostatic problem for point charges $+1,-1$ in a dielectric of $\varepsilon = 1$ inside the solute region (defined by the radii R^- and R^+: $R^- = R^+ = R_{vdw}(Cl^-)$) and $\varepsilon = \varepsilon_{el}$ outside. The Poisson equation was solved by the PCM[31] technique implemented in our code,[51] which has been extensively tested especially on the two-site system. The value of ε_{el} corresponding to the polarizable model[11] was found to be $\varepsilon_0/\varepsilon_{MD} = 1.62$. The nuclear part of the free energy ΔG_{nuc} was obtained in MD simulation using the CHARMM force field with scaled (by factor $1/\sqrt{1.62}$) charges of the ions.

The MD system consisted of two ions A^- and A^+ and 350 benzene molecules within the MD box with a ~38 Å edge. A prior computation has shown that all potential energy terms calculated for the same configuration of the system by two programs CHARMM (version c32b1) and Gromacs[52] coincide with each other to a high precision. For practical reasons, all simulations were carried out by the Gromacs[52] MD package; however, results are expected to be identical to a CHARMM simulation. The electrostatic interactions were treated by the PME technique with a real space cutoff of 12 Å. The new Berendsen thermostat with a stochastic term and a Berendsen barostat were used with the coupling constant 0.1 ps, to keep the temperature at 298 K and the pressure at 1 atm. For each separation distance r, the system was equilibrated first during a 1 ns run, followed by a 5 ns data collection run. The MD time step was 1 fs in the nonpolarizable and 0.5 fs in polarizable simulations. The positions of the Drude particles were optimized with a frequency of 1 fs in the self-consistent procedure as implemented in Gromacs.[52]

To quantify the screening effect, the value of ε was determined by fitting the function "$-1/\varepsilon r + \text{Ewald}(r)/\varepsilon +$ const" to the simulated PMF data. In the microscopic simulations, the const term appears due to some quadrupolar (nondielectric) and nonlinear contributions to the solvent polarization, but it does not essentially affect the force between the ions, $-\nabla U^{eff}(r)$, in the dielectric region ($r > R^- + R^+ + 2R_{solvent}$).

The comparison of PMF $U^{eff}(r)$ functions obtained with different force fields is shown in Figure 3. The shown PMF profiles are shifted by the corresponding values of the const, to reflect the correct boundary conditions at infinity, $U^{eff}(\infty) = 0$.

Fluctuations of Salt Bridges in Proteins. Cytochrome *c* oxidase is chosen as a probe protein due to its central role in energy metabolism in aerobic cells and our previous experience with this molecule. The enzyme is modeled by two subunits A and B taken from the fully reduced bovine heart cytochrome *c* oxidase structure (PDB code 1V55[53]). Additional water molecules were added between Glu-242 and the D channel, consistent with the *Rh. sphaeroides* structure.[54] The system was in the P_M state with Cu_A oxidized and heme *a* reduced. The partial charges of the redox centers, heme *a*, heme a_3, Cu_A, and Cu_B, are borrowed from ref 55, and the appropriate redox state was achieved by evenly distributing appropriate charge between metal ion and atoms directly coordinated to it. The structure was protonated according to the equilibrium protonation state of the residues determined previously.[48] The titratable residues with a proton occupancy larger than ~0.3 were treated as fully protonated, while all others as deprotonated, so as to avoid partial proton occupancies and the net charge on the molecule.

For MD simulations, Gromacs[52] with an AMBER force field ported by Eric J. Sorin[56] was used. The TIP3P model was used for water. It has been tested previously[44] that all potential energy terms calculated by the MD package AMBER7[57] and Gromacs for the same configuration of dehydrated C*c*O coincide with high precision.

The MD cell is formed by the protein immersed in a bath of water molecules and counterions K^+ and Cl^- with an effective salt concentration of 100 mM. The shortest distance from the protein to the edge of the MD box is 5 Å. Position restraints were applied to solvent exposed C_α atoms and membrane exposed heavy protein atoms. The electrostatic interactions were treated by the PME technique with a real space cutoff of 12 Å.

The new Berendsen thermostat with a stochastic term and coupling constant 0.3 ps was applied to keep the temperature at 298 K; also, the Berendsen pressure coupling with a reference pressure of 1 atm and a coupling constant of 0.5 ps was applied. All bonds to H atoms were constrained with the LINCS algorithm. The initial structure was energy-minimized and equilibrated in a 5 ns MD run before the sampling run. The sampling was collected in a 5 ns MD run with a 1 fs time step.

The interatomic distance d between O2D of Δ-propionate and 2HH2 of Arg438 (as shown in Figure 4) has been chosen to characterize the fluctuations of the salt bridge. The distribution functions of d are shown in Figure

5. Of particular interest for the C*c*O mechanism are configurations with large distances *d*; for such configurations, the water molecules from the internal cavity above the catalytic center can penetrate to the catalytic cavity of the enzyme, as shown in Figure 4.

References

(1) Cornell, W.; Cieplak, P.; Bayly, C.; Gould, I.; Merz, K.; Ferguson, D.; Spellmeyer, D.; Fox, T.; Caldwell, J.; Kollman, P. A second generation force field for the simulation of proteins, nucleic acids, and organic molecules. *J. Am. Chem. Soc.* **1995**, *117*, 5179–5197.

(2) Wang, J.; Cieplak, P.; Kollman, P. A. How well does a restrained electrostatic potential (RESP) model perform in calculating conformational energies of organic and biological molecules. *J. Comput. Chem.* **2000**, *21*, 1049–1074.

(3) Mackerell, A. D.; Bashford, D.; Bellott, M.; Dunbrack, R.; Evanseck, J.; Field, M.; Fischer, S.; Gao, J.; Guo, H.; Ha, S.; Joseph-McCarthy, D.; Kuchnir, L.; Kuczera, K.; Lau, F. T. K.; Mattos, C.; Michnick, S.; Ngo, T.; Nguyen, D. T.; Prodhom, B.; Reiher, W. E.; Roux, B.; Schlenkrich, M.; Smith, J. C.; Stote, R.; Straub, J.; Watanabe, M.; Wiorkiewicz-Kuczera, J.; Yin, D.; Karplus, M. All-Atom Empirical Potential for Molecular Modeling and Dynamics Studies of Proteins. *J. Phys. Chem. B* **1998**, *102*, 3586–3616.

(4) van Gunsteren, W. F.; Billeter, S. R.; Eising, A. A.; Hunenberger, P. H.; Kruger, P.; Mark, A. E.; Scott, W. R. P.; Tironi, I. G. *Biomolecular Simulation: The GROMOS96 Manual and User Guide*; Vdf Hochschulverlag AG an der ETH Zurich: Zurich, Switzerland, 1996.

(5) Jorgensen, W. L.; Maxwell, D. S.; Tirado-Rives, J. Development and Testing of the OPLS All-Atom Force Field on Conformational Energetics and Properties of Organic Liquids. *J. Am. Chem. Soc.* **1996**, *118*, 11225–11236.

(6) Frohlich, H. *Theory of Dielectrics*; Clarendon Press: Oxford, U.K., 1949.

(7) Rick, S. W.; Stuart, S. J.; Berne, B. J. Dynamical fluctuating charge force fields: Application to liquid water. *J. Chem. Phys.* **1994**, *101*, 6141–6156.

(8) Kaminski, G. A.; Stern, H. A.; Berne, B. J.; Friesner, R. A. Development of an Accurate and Robust Polarizable Molecular Mechanics Force Field from ab Initio Quantum Chemistry. *J. Phys. Chem. A* **2004**, *108*, 621–627.

(9) Patel, S.; Mackerell, A. D., Jr.; Brooks, C. L. CHARMM fluctuating charge force field for proteins: II Protein/solvent properties from molecular dynamics simulations using a nonadditive electrostatic model. *J. Comput. Chem.* **2004**, *25*, 1504–1514.

(10) Stuart, S. J.; Berne, B. J. Effects of Polarizability on the Hydration of the Chloride Ion. *J. Phys. Chem.* **1996**, *100*, 11934–11943.

(11) Lopes, P. E. M.; Lamoureux, G.; Roux, B.; MacKerell, A. D. Polarizable empirical force field for aromatic compounds based on the classical drude oscillator. *J. Phys. Chem. B* **2007**, *111*, 2873–2885.

(12) Anisimov, V. M.; Vorobyov, I. V.; Roux, B.; MacKerell, A. D., Jr. Polarizable Empirical Force Field for the Primary and Secondary Alcohol Series Based on the Classical Drude Model. *J. Chem. Theory Comput.* **2007**, *3*, 1927–1946.

(13) Vorobyov, I. V.; Anisimov, V. M.; MacKerell, A. D. Polarizable Empirical Force Field for Alkanes Based on the Classical Drude Oscillator Model. *J. Phys. Chem. B* **2005**, *109*, 18988–18999.

(14) Vorobyov, I.; Anisimov, V. M.; Greene, S.; Venable, R. M.; Moser, A.; Pastor, R. W.; MacKerell, A. D. Additive and Classical Drude Polarizable Force Fields for Linear and Cyclic Ethers. *J. Chem. Theory Comput.* **2007**, *3*, 1120–1133.

(15) Karplus, M. Molecular dynamics simulations of biomolecules. *Acc. Chem. Res.* **2002**, *35*, 321–323.

(16) Hummer, G.; Pratt, L. R.; Garcia, A. E. Free energy of ionic hydration. *J. Phys. Chem.* **1996**, *100*, 1206–1215.

(17) Oostenbrink, C.; Villa, A.; Mark, A. E.; Van Gunsteren, W. F. A biomolecular force field based on the free enthalpy of hydration and solvation: The GROMOS force-field parameter sets 53A5 and 53A6. *J. Comput. Chem.* **2004**, *25*, 1656–1676.

(18) Simonson, T.; Perahia, D. Internal and Interfacial Dielectric Properties of Cytochrome c from Molecular Dynamics in Aqueous Solution. *Proc. Natl. Acad. Sci. U. S. A.* **1995**, *92*, 1082–1086.

(19) Simonson, T.; Perahia, D. Microscopic Dielectric Properties of Cytochrome c from Molecular Dynamics Simulations in Aqueous Solution. *J. Am. Chem. Soc.* **1995**, *117*, 7987–8000.

(20) Halgren, T. A.; Damm, W. Polarizable force fields. *Curr. Opin. Struct. Biol.* **2001**, *11*, 236–242.

(21) Allen, T. W.; Andersen, O. S.; Roux, B. Molecular dynamics - potential of mean force calculations as a tool for understanding ion permeation and selectivity in narrow channels. *Biophys. Chem.* **2006**, *124*, 251–267.

(22) Gao, J. L.; Truhlar, D. G. Quantum mechanical methods for enzyme kinetics. *Annu. Rev. Phys. Chem.* **2002**, *53*, 467–505.

(23) Senn, H. M.; Thiel, W. QM/MM Methods for Biomolecular Systems. *Angew. Chem., Int. Ed.* **2009**, *48*, 1198–1229.

(24) Vener, M. V.; Leontyev, I. V.; Basilevsky, M. V. Computations of solvation free energies for polyatomic ions in water in terms of a combined molecular-continuum approach. *J. Chem. Phys.* **2003**, *119*, 8038–8046.

(25) Leontyev, I. V.; Stuchebrukhov, A. A. Electronic continuum model for molecular dynamics simulations. *J. Chem. Phys.* **2009**, *130*, 085102.

(26) Guillot, B. A reappraisal of what we have learnt during three decades of computer simulations on water. *J. Mol. Liq.* **2002**, *101*, 219–260.

(27) Jorgensen, W. L.; Chandrasekhar, J.; Madura, J. D.; Impey, R. W.; Klein, M. L. Comparison of Simple Potential Functions for Simulating Liquid Water. *J. Chem. Phys.* **1983**, *79*, 926–935.

(28) Berendsen, H. J. C.; Grigera, J. R.; Straatsma, T. P. The Missing Term in Effective Pair Potentials. *J. Phys. Chem.* **1987**, *91*, 6269–6271.

(29) Platzman, R.; Franck, J. The Role of the Hydration Configuration in Electronic Processes Involving Ions in Aqueous Solution. *Z. Phys.* **1954**, *138*, 411–431.

(30) Schutz, C. N.; Warshel, A. What are the dielectric constants of proteins and how to validate electrostatic models. *Proteins* **2001**, *44*, 400–417.

(31) Miertus, S.; Scrocco, E.; Tomasi, J. Electrostatic Interaction of a Solute with a Continuum - a Direct Utilization of Abinitio Molecular Potentials for the Prevision of Solvent Effects. *Chem. Phys.* **1981**, *55*, 117–129.

(32) Vener, M. V.; Tovmash, A. V.; Rostov, I. V.; Basilevsky, M. V. Molecular Simulations of Outersphere Reorganization Energies in Polar and Quadrupolar Solvents. The Case of Intramolecular Electron and Hole Transfer. *J. Phys. Chem. B* **2006**, *110*, 14950–14955.

(33) Geerke, D. P.; van Gunsteren, W. F. Force Field Evaluation for Biomolecular Simulation: Free Enthalpies of Solvation of Polar and Apolar Compounds in Various Solvents. *ChemPhysChem* **2006**, *7*, 671–678.

(34) Neumann, M.; Steinhauser, O. Computer simulation and the dielectric constant of polarizable polar systems. *Chem. Phys. Lett.* **1984**, *106*, 563–569.

(35) Simonson, T.; Brooks, C. L. Charge Screening and the Dielectric Constant of Proteins: Insights from Molecular Dynamics. *J. Am. Chem. Soc.* **1996**, *118*, 8452–8458.

(36) Badyal, Y. S.; Saboungi, M. L.; Price, D. L.; Shastri, S. D.; Haeffner, D. R.; Soper, A. K. Electron distribution in water. *J. Chem. Phys.* **2000**, *112*, 9206–9208.

(37) Silvestrelli, P. L.; Parrinello, M. Structural, electronic, and bonding properties of liquid water from first principles. *J. Chem. Phys.* **1999**, *111*, 3572–3580.

(38) Sharma, M.; Resta, R.; Car, R. Dipolar correlations and the dielectric permittivity of water. *Phys. Rev. Lett.* **2007**, *98*, 247401.

(39) Delle Site, L.; Lynden-Bell, R. M.; Alavi, A. What can classical simulators learn from ab initio simulations? *J. Mol. Liq.* **2002**, *98*−*9*, 79–86.

(40) Kirkwood, J. G. The dielectric polarization of polar liquids. *J. Chem. Phys.* **1939**, *7*, 911–919.

(41) Simonson, T.; Carlsson, J.; Case, D. Proton Binding to Proteins: pKa Calculations with Explicit and Implicit Solvent Models. *J. Am. Chem. Soc.* **2004**, *126*, 4167–4180.

(42) Archontis, G.; Simonson, T. Proton Binding to Proteins: A Free-Energy Component Analysis Using a Dielectric Continuum Model. *Biophys. J.* **2005**, *88*, 3888–3904.

(43) Vorobyov, I.; Li, L.; Allen, T. W. Assessing Atomistic and Coarse-Grained Force Fields for Protein? Lipid Interactions: the Formidable Challenge of an Ionizable Side Chain in a Membrane. *J. Phys. Chem. B* **2008**, *112*, 9588–9602.

(44) Leontyev, I. V.; Stuchebrukhov, A. A. Dielectric relaxation of cytochrome c oxidase: Comparison of the microscopic and continuum models. *J. Chem. Phys.* **2009**, *130*, 085103.

(45) Frisch, M. J.; Trucks, G. W.; Schlegel, H. B. G. E.; Scuseria, M. A.; Robb, J. R.; Cheeseman, J. A.; Montgomery, J. T.; Vreven, K. N.; Kudin, J. C.; Burant, J. M.; Millam, S. S.; Iyengar, J.; Tomasi, V.; Barone, B.; Mennucci, M.; Cossi, G.; Scalmani, N.; Rega, G. A.; Petersson, H.; Nakatsuji, M.; Hada, M.; Ehara, K.; Toyota, R.; Fukuda, J.; Hasegawa, M.; Ishida, T.; Nakajima, Y.; Honda, O.; Kitao, H.; Nakai, M.; Klene, X.; Li, J. E.; Knox, H. P.; Hratchian, J. B.; Cross, C.; Adamo, J.; Jaramillo, R.; Gomperts, R. E.; Stratmann, O.; Yazyev, A. J.; Austin, R.; Cammi, C.; Pomelli, J. W.; Ochterski, P. Y.; Ayala, K.; Morokuma, G. A.; Voth, P.; Salvador, J. J.; Dannenberg, V. G.; Zakrzewski, S.; Dapprich, A. D.; Daniels, M. C.; Strain, O.; Farkas, D. K.; Malick, A. D.; Rabuck, K.; Raghavachari, J. B.; Foresman, J. V.; Ortiz, Q.; Cui, A. G.; Baboul, S.; Clifford, J.; Cioslowski, B. B.; Stefanov, G.; Liu, A.; Liashenko, P.; Piskorz, I.; Komaromi, R. L.; Martin, D. J.; Fox, T.; Keith, M. A.; Al-Laham, C. Y.; Peng, A.; Nanayakkara, M.; Challacombe, P. M. W.; Gill, B.; Johnson, W.; Chen, M. W.; Wong, C.; Gonzalez, C.; Pople, J. A. *Gaussian 03*, revision B.04; Gaussian, Inc.: Pittsburgh, PA, 2003.

(46) Lide, D. R. *CRC Handbook of Chemistry and Physics*, 84th ed.; CRC Press/Taylor and Francis: Boca Raton, FL, 2003.

(47) Hochtl, P.; Boresch, S.; Bitomsky, W.; Steinhauser, O. Rationalization of the dielectric properties of common three-site water models in terms of their force field parameters. *J. Chem. Phys.* **1998**, *109*, 4927–4937.

(48) Popovic, D. M.; Stuchebrukhov, A. A. Electrostatic Study of the Proton Pumping Mechanism in Bovine Heart Cytochrome c Oxidase. *J. Am. Chem. Soc.* **2004**, *126*, 1858–1871.

(49) Wikstrom, M.; Ribacka, C.; Molin, M.; Laakkonen, L.; Verkhovsky, M.; Puustinen, A. Gating of proton and water transfer in the respiratory enzyme cytochrome c oxidase. *Proc. Natl. Acad. Sci. U. S. A.* **2005**, *102*, 10478–10481.

(50) Zhu, K.; Shirts, M. R.; Friesner, R. A. Improved Methods for Side Chain and Loop Predictions via the Protein Local Optimization Program: Variable Dielectric Model for Implicitly Improving the Treatment of Polarization Effects. *J. Chem. Theory Comput.* **2007**, *3*, 2108–2119.

(51) Vener, M. V.; Leontyev, I. V.; Dyakov, Y. A.; Basilevsky, M. V.; Newton, M. D. Application of the Linearized MD Approach for Computing Equilibrium Solvation Free Energies of Charged and Dipolar Solutes in Polar Solvents. *J. Phys. Chem. B* **2002**, *106*, 13078–13088.

(52) van der Spoel, D.; Lindahl, E.; Hess, B.; van Buuren, A. R.; Apol, E.; Meulenhoff, P. J.; Tieleman, D. P.; Sijbers, A. L. T. M.; Feenstra, K. A.; van Drunen, R.; Berendsen, H. J. C. Gromacs User Manual version 4.0, www.gromacs.org (accessed Mar 2010).

(53) Tsukihara, T.; Shimokata, K.; Katayama, Y.; Shimada, H.; Muramoto, K.; Aoyama, H.; Mochizuki, M.; Shinzawa-Itoh, K.; Yamashita, E.; Yao, M.; Ishimura, Y.; Yoshikawa, S. The low-spin heme of cytochrome c oxidase as the driving element of the proton-pumping process. *Proc. Natl. Acad. Sci. U. S. A.* **2003**, *100*, 15304–15309.

(54) Qin, L.; Hiser, C.; Mulichak, A.; Garavito, R. M.; Ferguson-Miller, S. Identification of conserved lipid/detergent-binding sites in a high-resolution structure of the membrane protein cytochrome c oxidase. *Proc. Natl. Acad. Sci. U. S. A.* **2006**, *103*, 16117–16122.

(55) Tashiro, M.; Stuchebrukhov, A. A. Thermodynamic Properties of Internal Water Molecules in the Hydrophobic Cavity around the Catalytic Center of Cytochrome c Oxidase. *J. Phys. Chem. B* **2005**, *109*, 1015–1022.

(56) Sorin, E. J.; Pande, V. S. Exploring the Helix-Coil Transition via All-Atom Equilibrium Ensemble Simulations. *Biophys. J.* **2005**, *88*, 2472–2493.

(57) Case, D. A.; Pearlman, D. A.; Caldwell, J. W.; Cheatham, T. E., III; Wang, J.; Ross, W. S.; Simmerling, C. L.; Darden, T. A.; Merz, K. M.; Stanton, R. V.; Cheng, A. L.; Vincent, J. J.; Crow-ley, M.; Tsui, V.; Gohlke, H.; Radmer, R. J.; Duan, Y.; Pitera, J.; Massova, I.; Seibel, G. L.; Singh, U. C.; Weiner, P. K.; Kollman, P. A. *AMBER 7 Users' Manual.*: University of California: San Francisco, 2002.

CT9005807